

# Effects of the randomly distributed magnetic field on the phase diagrams of the Ising Nanowire II: continuous distributions

Ümit Akıncı<sup>1</sup>

*Department of Physics, Dokuz Eylül University, TR-35160 Izmir, Turkey*

## 1 Abstract

The effect of the random magnetic field distribution on the phase diagrams and ground state magnetizations of the Ising nanowire has been investigated with effective field theory with correlations. Gaussian distribution has been chosen as a random magnetic field distribution. The variation of the phase diagrams with that distribution parameters has been obtained and some interesting results have been found such as disappearance of the reentrant behavior and first order transitions which appear in the case of discrete distributions. Also for single and double Gaussian distributions, ground state magnetizations for different distribution parameters have been determined which can be regarded as separate partially ordered phases of the system. Keywords: **Ising Nanowire; random magnetic field; Gaussian magnetic field distribution**

## 2 Introduction

Recently there has been growing interest both theoretically and experimentally in the magnetic nanomaterials such as nanoparticles, nanorods, nanotubes and nanowires. Nowadays, fabrication of these nanomaterials is no longer difficult, since development of the experimental techniques permits us making materials with a few atoms. For instance, acicular magnetic nano elements were already fabricated [1, 2, 3] and magnetization of the nanomaterial has been measured [4]. Nanoparticle systems have growing application areas, e.g. they can be used as sensors [5], permanent magnets [6], beside some medical applications [7]. In particular, magnetic nanowires and nanotubes have many applications in nanotechnology [8, 9]. Nanowires can be used as an ultrahigh density magnetic recording media [10, 11, 12] and they have potential applications in biotechnology [13, 14], such as Ni nanowires can be used for bio separation [15, 16].

In the nanometer scale, physical properties of these finite materials are different from those of their bulk counterparts. Some properties of these materials, which highly depend on the size and the dimensionality, can be used for fabrication of materials for various purposes. From this point of view, it is important to determine the properties of these materials theoretically. Most common used theoretical methods for determining the magnetic properties of these materials are mean field approximation (MFA), effective field theory (EFT) and Monte Carlo (MC) simulation as in bulk systems. For instance, nanoparticles investigated by EFT with correlations [17], MFA and MC [18]. The phase diagrams and the magnetizations of the nanoparticle described by the transverse Ising model have been investigated by using MFA and EFT [19, 20]. Moreover, investigation of compensation temperature of the nanoparticle [21] and magnetic properties of the nanocube with MC [22] are among these studies.

Another method, namely variational cumulant expansion (VCE) based on expanding the free energy in terms of the action up to  $m^{th}$  order, has been applied to the magnetic superlattices [23] and ferromagnetic nanoparticles [24, 25]. The first order expansion within this method gives the results of the MFA.

Various nano structures can be modeled by core-shell models and these models can be solved also by MFA, EFT and MC such as *FePt* and *Fe<sub>3</sub>O<sub>4</sub>* nanotubes [26]. The phase diagrams and magnetizations of the transverse Ising nanowire has been treated within MFA and EFT [27, 28], the effect of the surface dilution on the magnetic properties of the cylindrical Ising nanowire and nanotube has been studied [29, 30], the magnetic properties of nanotubes of different diameters, using armchair or zigzag edges has been investigated with MC [31], initial susceptibility of the Ising nanotube and nanowire have been calculated within the EFT with correlations [32, 33] and the

---

<sup>1</sup>umit.akinci@deu.edu.tr

compensation temperature which appears for negative core-shell coupling has been investigated by EFT for nanowire and nanotube [34]. There are also some works dealing with hysteresis characteristics of the cylindrical Ising nanowire [35, 36]. Beside these, higher spin nanowire or nanotube systems have also been investigated, such as spin-1 nanotube [37] and nanowire [38], mixed spin - 3/2, 1 core shell structured nanoparticle [39], mixed spin - 1/2, 1 nanotube [40] systems.

On the other hand, as far as we know, there have less attention paid on quenched randomness effects on these systems, except the site dilution. However, including quenched randomness or disorder effects in these systems may induce some beneficial results. For this purpose we investigate the effects of the random magnetic field distributions on the phase diagrams of the Ising nanowire within this work. As stated in [29] the phase diagrams of the nanotube and nanowire are qualitatively similar, then investigation of the effect of the random magnetic field distribution on the nanowire will give hints about the effect of the same distribution on the phase diagrams of the nanotube.

The Ising model in a quenched random field (RFIM) has been studied over three decades. The model which is actually based on the local fields acting on the lattice sites which are taken to be random according to a given probability distribution was introduced for the first time by Larkin [41] for superconductors and later generalized by Imry and Ma [42]. Beside the similarities between diluted antiferromagnets in a homogenous magnetic field and ferromagnetic systems in the presence of random fields [43, 44], the importance of the random field distributions on these systems comes from the fact that, random distribution of the magnetic field drastically affects the phase diagrams of the system, and hence the magnetic properties. This situation has been investigated widely in the literature for the bulk Ising systems. For example, using a Gaussian probability distribution, Schneider and Pytte [45] have shown that phase diagrams of the model exhibit only second order phase transition properties. On the other hand, Aharony [46] and Mattis [47] have introduced bimodal and trimodal distributions, respectively, and they have reported the observation of tricritical behavior. With the same distributions and using EFT with correlations, Borges and Silva [48, 49, 50] showed that three dimensional lattices show tricritical behavior while two dimensional lattices do not exhibit this behavior. On the other hand, by using two site EFT instead of one site EFT, tricritical behavior can be observed on a square lattice [51]. Similarly, Sarmiento and Kaneyoshi [52] investigated the phase diagrams of RFIM by means of EFT with correlations for a bimodal field distribution, and they concluded that reentrant behavior of second order is possible for a system with ( $q \geq 6$ ). Recently, Fytas et al. [53] applied MC simulations on a simple cubic lattice. They found that the transition is continuous for a bimodal field distribution, while Hadjiagapiou [54] observed reentrant behavior and confirmed the existence of a tricritical point for an asymmetric bimodal probability distribution within the MFA based on a Landau expansion.

In a recent series of papers, phase transition properties of infinite dimensional RFIM with symmetric double [55] and triple [56] Gaussian random fields have also been studied by means of a replica method and a rich variety of phase diagrams have been presented. The situation has also been handled on 3D lattices with nearest-neighbor interactions by a variety of theoretical works such as EFT [57, 58], EFT with multi site spin correlations [59], MC simulations [60, 61, 62], pair approximation [63], and the series expansion method [64].

As seen in the short literature in bulk Ising systems, random field distributions keep up to date in the literature. Thus the aim of this work is to inspect the effects of random field distributions on the phase diagrams of the nanowire system as a nanostructure. The paper is organized as follows: In Sec. 3 we briefly present the model and formulation. The results and discussions are presented in Sec. 4, and finally Sec. 5 contains our conclusions.

### 3 Model and Formulation

We consider a nanowire which has geometry shown in Fig. 1. The Hamiltonian of the nanowire is given by

$$\mathcal{H} = -J_1 \sum_{\langle i,j \rangle} s_i s_j - J_2 \sum_{\langle m,n \rangle} s_m s_n - J_3 \sum_{\langle i,m \rangle} s_i s_m - \sum_i H_i s_i - \sum_m H_m s_m \quad (1)$$

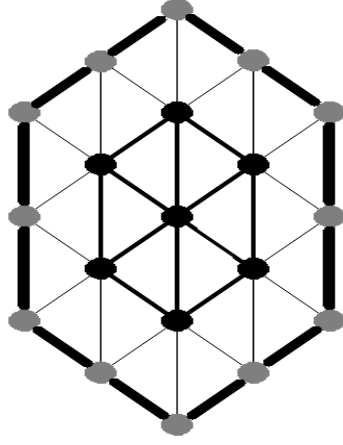


Figure 1: Schematic representation of a cylindrical nanowire (top view). The gray/black circles represent the surface/shell magnetic atoms, respectively.

where  $s_i$  is the  $z$  component of the spin at a lattice site  $i$  and it takes the values  $s_i = \pm 1$  for the spin-1/2 system.  $J_1$  and  $J_2$  are the exchange interactions between spins which are located at the core and shell, respectively, and  $J_3$  is the exchange interaction between the core and shell spins which are nearest neighbor to each other.  $H_i$  and  $H_m$  are the external longitudinal magnetic fields at the lattice sites  $i$  and  $m$  respectively. Magnetic fields are distributed on the lattice sites according to a given probability distribution. The first three summations in Eq. (1) are over the nearest-neighbor pairs of spins, and the other summations are over all the lattice sites.

This work -as a continuation of the earlier work [69]- deals with the following continuous magnetic field distribution,

$$P(H_i) = pG(0, \sigma) + \frac{1-p}{2} [G(H_0, \sigma) + G(-H_0, \sigma)] \quad (2)$$

where  $G(H_0, \sigma)$  is the Gaussian distribution centered at  $H_0$  with a width  $\sigma$  and it is given by

$$G(H_0, \sigma) = \left( \frac{1}{2\pi\sigma^2} \right)^{1/2} \exp \left[ -\frac{(H_i - H_0)^2}{2\sigma^2} \right]. \quad (3)$$

Distribution given in Eq. (2) reduces to the system with zero magnetic field (pure system) for  $p = 1, \sigma = 0$ . According to the distribution given in Eq. (2),  $p$  percentage of the lattice sites are subjected to a magnetic field chosen from the Gaussian distribution which has  $\sigma$  width and  $H_0 = 0$  as a center. Half of the remaining sites are under the influence of a field  $H_i$  which is randomly chosen from the magnetic field distribution  $G(H_0, \sigma)$ , whereas the distribution  $G(-H_0, \sigma)$  used as distribution function on the remaining sites.

Four different representative magnetizations ( $m_i, i = 1, 2, 3, 4$ ) for the system can be given by usual EFT equations which are obtained by differential operator technique and decoupling approximation (DA) [65, 66],

$$\begin{aligned} m_1 &= [A_1 + m_1 B_1]^4 [A_3 + m_2 B_3] [A_3 + m_3 B_3]^2 [A_1 + m_4 B_1] \\ m_2 &= [A_3 + m_1 B_3] [A_2 + m_2 B_2]^2 [A_2 + m_3 B_2]^2 \\ m_3 &= [A_3 + m_1 B_3]^2 [A_2 + m_2 B_2]^2 [A_2 + m_3 B_2]^2 \\ m_4 &= [A_1 + m_1 B_1]^6 [A_1 + m_4 B_1]^2 \end{aligned} \quad (4)$$

Here  $m_1, m_4$  are the magnetizations of the two different representative sites in the core and  $m_2, m_3$  are the magnetizations of the two different representative sites in the shell. The coefficients in the expanded form of Eq. (4) are given by

$$A_p^k A_q^l B_p^m B_q^n = \int dH_i P(H_i) \cosh^k(J_p \nabla) \cosh^l(J_q \nabla) \sinh^m(J_p \nabla) \sinh^n(J_q \nabla) f(H_i, x) |_{x=0} \quad (5)$$

where  $\nabla$  is the usual differential operator in the differential operator technique and the values of indices  $p, q$  can be  $p, q = 1, 2, 3$ . The function is defined by

$$f(H_i, x) = \tanh(\beta x + \beta H_i). \quad (6)$$

as usual for the spin-1/2 system. In Eq. (6),  $\beta = 1/(k_B T)$  where  $k_B$  is Boltzmann constant and  $T$  is the temperature. The effect of the exponential differential operator to an arbitrary function  $F(x)$  is given by

$$\exp(a\nabla)F(x) = F(x+a) \quad (7)$$

with any constant  $a$ . DA will give the results of the Zernike approximation [67] for this system.

With the help of the Binomial expansion, Eq. (4) can be written in the form

$$\begin{aligned} m_1 &= \sum_{i=0}^4 \sum_{j=0}^1 \sum_{k=0}^2 \sum_{l=0}^1 K_1(i, j, k, l) m_1^i m_2^j m_3^k m_4^l \\ m_2 &= \sum_{i=0}^1 \sum_{j=0}^2 \sum_{k=0}^2 K_2(i, j, k) m_1^i m_2^j m_3^k \\ m_3 &= \sum_{i=0}^2 \sum_{j=0}^2 \sum_{k=0}^2 K_3(i, j, k) m_1^i m_2^j m_3^k \\ m_4 &= \sum_{i=0}^6 \sum_{l=0}^2 K_4(i, l) m_1^i m_4^l \end{aligned} \quad (8)$$

where

$$\begin{aligned} K_1(i, j, k, l) &= \binom{4}{i} \binom{2}{k} A_1^{5-i-l} A_3^{3-j-k} B_1^{i+l} B_3^{j+k} \\ K_2(i, j, k) &= \binom{2}{j} \binom{2}{k} A_2^{4-j-k} A_3^{1-i} B_2^{j+k} B_3^i \\ K_3(i, j, k) &= \binom{2}{i} \binom{2}{j} \binom{2}{k} A_2^{4-j-k} A_3^{2-i} B_2^{j+k} B_3^i \\ K_4(i, l) &= \binom{6}{i} \binom{2}{l} A_1^{8-i-l} B_1^{i+l} \end{aligned} \quad (9)$$

These coefficients can be calculated from the definitions given in Eq. (5) with using Eq. (7).

For a given Hamiltonian and field distribution parameters, by determining the coefficients from Eq. (9) we can obtain a system of coupled non linear equations from Eq. (8), and by solving this system we can get the magnetizations  $m_i, i = 1, 2, 3, 4$ . The magnetization of the core ( $m_c$ ) and shell ( $m_s$ ) of nanowire, as well as the total magnetization ( $m_T$ ) can be calculated via

$$m_c = \frac{1}{7}(6m_1 + m_4), \quad m_s = \frac{1}{12}(6m_2 + 6m_3), \quad m_T = \frac{1}{19}(6m_1 + 6m_2 + 6m_3 + m_4) \quad (10)$$

Since in the vicinity of the critical point all magnetizations are close to zero, we can obtain another coupled equation system for determining this critical point by linearizing the equation system given in Eq. (8), i.e.

$$A \cdot m = 0 \quad (11)$$

where

$$A = \begin{pmatrix} K_1(1, 0, 0, 0) - 1 & K_1(0, 1, 0, 0) & K_1(0, 0, 1, 0) & K_1(0, 0, 0, 1) \\ K_2(1, 0, 0) & K_2(0, 1, 0) - 1 & K_2(0, 0, 1) & 0 \\ K_3(1, 0, 0) & K_3(0, 1, 0) & K_3(0, 0, 1) - 1 & 0 \\ K_4(1, 0) & 0 & 0 & K_4(0, 1) - 1 \end{pmatrix} \quad (12)$$

$$m = \begin{pmatrix} m_1 \\ m_2 \\ m_3 \\ m_4 \end{pmatrix}. \quad (13)$$

Critical temperature can be determined from  $\det(A) = 0$ . As discussed in [33], the matrix  $A$  given in Eq. (12) is invariant under the transformation  $J_3 \rightarrow -J_3$  then we can conclude that the system with ferromagnetic ( $J_3 > 0$ ) core-shell interaction has the same critical temperature as that of the system with anti-ferromagnetic ( $J_3 < 0$ ) core-shell interaction (with the same  $|J_3|$ ) for certain Hamiltonian and magnetic field distribution parameters. Although this discussion has been made for the system with zero magnetic field in [33], this conclusion is also valid for this system, because of the symmetry of the magnetic field distribution. Equation  $\det(A) = 0$  is invariant under the transformation  $J_3 \rightarrow -J_3$  for the nanowire with magnetic field distribution given in Eq. (2).

Beside this, there are some symmetry properties of the coefficients defined by Eq. (9). Although the numerical integration in Eq. (5) do not take too much time, using these symmetry properties will shorten the numerical calculation time. These symmetry properties can be found in Sec. 6.

## 4 Results and Discussion

In this section we discuss the effect of the continuous random magnetic field distribution on the phase diagrams of the system. Since the phase diagrams are the same for the  $J_3 > 0$  and  $J_3 < 0$  with the same  $|J_3|$ , we focus ourselves on the case  $J_3 > 0$ , i.e. ferromagnetic core-shell interaction. We use the scaled interactions as

$$J_1 = J, \quad r_n = \frac{J_n}{J}, \quad n = 2, 3. \quad (14)$$

We start with a single Gaussian magnetic field distribution.

### 4.1 Single Gaussian Distribution

The form of single Gaussian distribution which is defined in Eq. (2) is governed by only one parameter  $\sigma$ , which is the width of the distribution. This distribution distributes negative and positive valued magnetic fields -which are chosen from the Gaussian distribution- to lattice sites so that sum of all lattice site's magnetic field is equal to zero. Although the total magnetic field is zero, randomly distributed negative and positive fields drag the system to the disordered phase. On the other hand, the interactions  $J_n, (n = 1, 2, 3)$  enforce the system to stay in the ordered phase. Another factor is the temperature which causes thermal agitations which induce disordered phase when energy supplied by the temperature to the system is high enough. Thus a competition takes place between these factors.

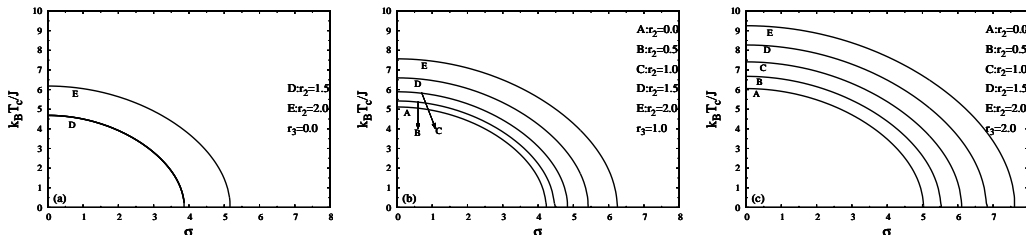


Figure 2: The phase diagrams of the nanowire with single Gaussian random field distribution in the  $(k_B T_c / J, \sigma)$  plane for different  $r_2, r_3$  values.

The phase diagrams in  $(k_B T_c / J, \sigma)$  plane can be seen in Fig. 2 for different  $r_2$  and  $r_3$  values. Firstly we can see from Fig. 2 that the general effect of increasing  $\sigma$  is to decrease the critical temperature, as expected. There is not any evidence of reentrant behavior in the phase diagrams, as in ordinary Ising lattices[68]. The critical temperature value at  $\sigma = 0$  and the critical value of the  $\sigma$ -which makes the critical temperature zero- depend on  $r_2, r_3$ , i.e. when  $r_2$  or  $r_3$  raises, these two critical values gets higher except one region. As in the same system with discrete distributions [69] when  $r_3 = 0.0$  up to a certain value of the  $r_2$ , the phase diagrams are the same in  $(k_B T_c / J, \sigma)$  plane. In Fig. 2(a) all phase diagrams are the same for  $r_2 \leq 1.5$ . This fact can be explained by

taking into account the total spin-spin interaction strengths of the core and shell which do not interact with each other when  $r_3 = 0.0$ .

In the absence of the interaction between the core and shell, the critical temperature of the system is determined by the core, up to a certain  $r_2 > 1.0$  value. Two distinct shell spins (which have magnetizations  $m_2, m_3$ ) have four nearest neighbors, and two distinct core spins (magnetizations of which are labeled as  $m_1, m_4$ ) have five and eight nearest neighbors, respectively. Thus at the value of  $r_2 = 1.0$ , core has higher critical temperature than the shell. As  $r_2$  increases, the critical temperature of the shell gets higher and after a certain value of  $r_2$ , the shell begins to determine the critical temperature of the system. Before this value, changing  $r_2$  can not change the phase diagrams of the system. The dependence of the critical temperature values of the core and shell can be seen in variation of their magnetization curves with temperature which are given in Fig. 3 for some selected values of  $r_2$  with fixed  $r_3 = 0.0$  and  $\sigma = 3.0$  values.

Within this region, although increasing  $r_2$  does not change the critical temperature of the system for a fixed value of  $\sigma$ , it causes change in the magnetization behavior with the temperature as seen in Fig. 3(c). As seen in Fig. 3(b), as  $r_2$  increases for a fixed  $\sigma$ , the ground state magnetization and the critical temperature of the shell layer increase. When  $r_2$  reaches the value that makes the critical temperature of the shell equal to the critical temperature of the core, increasing  $r_2$  after this value manifests itself in rising critical temperature of the system.

We can see from Fig. 2 that, increasing  $r_2$  and  $r_3$  values make the ferromagnetic region wider in  $(k_B T_c / J, \sigma)$  plane (except for the region explained above), since increasing  $r_2$  and  $r_3$  values raises the absolute value of the lattice energy coming from the spin-spin interaction, which must be overcome by both thermal agitations and random magnetic fields for the phase transition from an ordered phase to a disordered one.

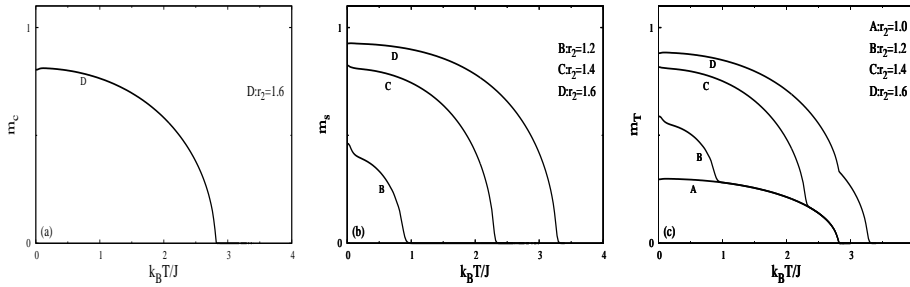


Figure 3: Variation of the magnetization with temperature for some selected  $r_2$  values of the nanowire with single Gaussian random field distribution. The fixed parameter values are  $r_3 = 0.0, \sigma = 3.0$ .

As we done in our earlier work [69] for discrete distributions, now we want to investigate the variation of ground state magnetization behaviors with  $\sigma$ . Then our question is; how the ground state magnetizations change as  $\sigma$  is varied for different  $r_2, r_3$  values? We know from the conclusions of our earlier work [69], bimodal and trimodal discrete random magnetic field distributions produces a number of ground state magnetizations which are different from zero (disordered phase) and one (ordered phase). These intermediate states may be regarded as partially ordered phases. In Fig. 4, we plot the variation of the ground state magnetization values ( $m_c^g, m_s^g, m_T^g$  core, shell and total ground state magnetization, respectively) as a function of the width of the single Gaussian distribution ( $\sigma$ ) for some selected values of  $r_2$  with  $r_3 = 1.0$ . We can see from the Fig. 4 that, this distribution creates higher number of these partially ordered phases, in comparison with the discrete distributions. Although increasing  $\sigma$  decreases the critical temperature of the system gradually as seen in Fig. (2), EFT based on DA approximation gives that, increasing  $\sigma$  decreases the ground state magnetization as a general trend, but it creates some plateaus i.e. there are some regions where the ground state magnetizations does not change with varying  $\sigma$  values. With increasing temperature, the effect of the increasing  $\sigma$  on the magnetization becomes continuous i.e. increasing  $\sigma$  decreases the magnetization continuously at higher temperatures as seen again in

Fig. 4.

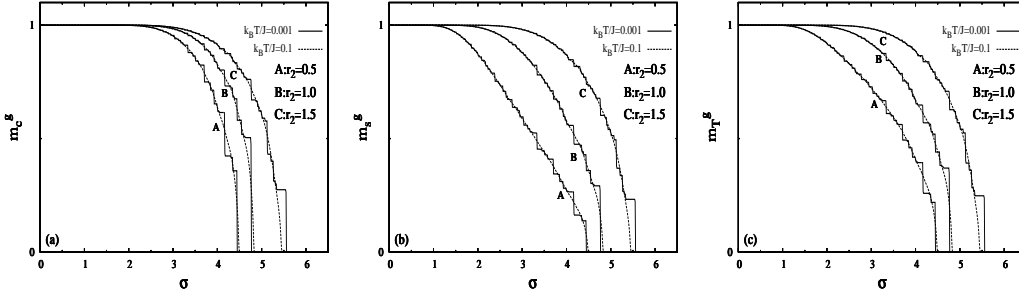


Figure 4: Variation of the ground state magnetizations with  $\sigma$  for some selected values of  $r_2$  for the system with single Gaussian magnetic field distribution. Each magnetization calculated at a temperature  $k_B T/J = 0.001$  can be regarded as ground state of the system. At the same time, the magnetization values calculated at the temperature  $k_B T/J = 0.1$  are plotted as dashed lines with the same  $r_2$  values. Fixed parameter value is  $r_3 = 1.0$ .

## 4.2 Double Gaussian Distribution

Let us investigate the phase diagrams of the nanowire with double Gaussian distribution. This distribution is given by Eq. (2) with  $p = 0$ . In Fig. 5, we plot the phase diagrams in the  $(k_B T_c/J, H_0/J)$  plane for some selected  $r_2, r_3$  and  $\sigma$  values. First, we see from the Fig. 5 that, for fixed  $r_2, r_3$  and  $\sigma$  values, when the distance between the centers of the Gaussians ( $2H_0/J$ ) increases, the critical temperature of the system gets smaller. Beside this, for fixed  $r_2, r_3$  values, increasing  $\sigma$  makes the ferromagnetic region in the  $(k_B T_c/J, H_0/J)$  plane narrower, since the randomness increases due to increasing  $\sigma$ . Another effect of the rising  $\sigma$  in this distribution is that, increasing  $\sigma$  destroys the reentrant behavior which exist in the system for given  $r_2, r_3$  values for the bimodal distribution (i.e. double Gaussian distribution with  $\sigma = 0.0$ ) as seen in Figs. 5(a),(d),(e),(f). Not only reentrant behavior disappears when  $\sigma$  rises, but also first order transitions and tricritical points. At the same time as seen in Figs. 5(b) and (c), rising  $\sigma$  also destroys other first order transitions which originate from an ordered phase to a disordered phase and which may not come with the reentrant behavior. Then we can say that for the nanowire, while bimodal distribution can induce a first order transitions -and also tricritical points- at higher  $H_0/J$  values, double Gaussian distribution can destroy these first order transitions when  $\sigma$  is large enough.

The ground state magnetizations appear in more complicated forms for this distribution than those corresponding to the bimodal distribution[69]. This can be seen from Fig. 6 which represents the ground state magnetizations corresponding to the phase diagrams given in Fig. 5(c). As in the single Gaussian distribution, large number of partially ordered phases appear in the system which disappear when the temperature rises.

## 5 Conclusion

In this work, the effect of the continuous random magnetic field distributions on the phase diagrams and ground state magnetizations of the Ising nanowire has been investigated.

There are two distribution parameters ( $H_0/J$  and  $\sigma$ ) of the random magnetic fields which can also be regarded as degree of the randomness which is imposed by the distribution of the magnetic field on the nanowire. Rising  $H_0/J$  or  $\sigma$  can be considered as higher degree of randomness. This shows itself as a change in the phase diagrams which are plotted in  $(k_B T_c/J - \sigma)$  or  $(k_B T_c/J - H_0/J)$  planes. We can say that, this change is two fold when we compare the results of the continuous distribution with the discrete distribution. First one is obvious; the ferromagnetic region in that planes collapses with rising degree of randomness. The second one is, rising degree of randomness imposed by rising  $\sigma$  on the system, destroys all first order transition lines and also tricritical points

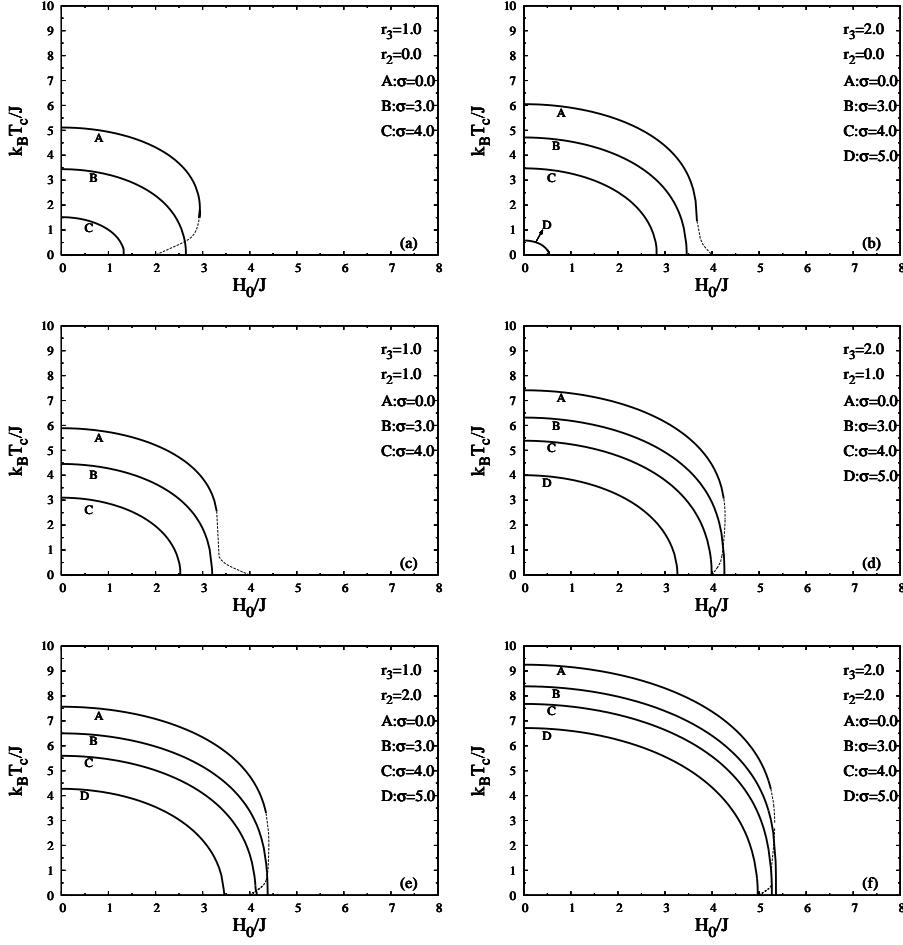


Figure 5: The phase diagrams of the nanowire with double Gaussian random field distribution in the  $(k_B T_c/J, H_0/J)$  plane for different  $r_2, r_3, \sigma$  values

at which the first order and second order transition lines meet. Rising degree of randomness which is caused by rising  $\sigma$ , also destroys reentrant behavior. While the system with magnetic field distribution given in Eq. (2) with  $\sigma = 0.0$  can show reentrant behavior, after a certain  $\sigma$ -which depends on  $r_2$  and  $r_3$ - this behavior disappears. This means that, the system with double Gaussian distribution can not pass the border of the two phases with thermal agitations from a disordered phase to an ordered phase after a certain  $\sigma$  value.

Rising degree of randomness also shows itself in the ground state magnetizations. As one can see in [69], bimodal magnetic field distribution can induce a few plateaus in the  $(m_T^g - K_B T/J)$  plane. These plateaus where the ground state magnetization values do not change with rising randomness can be regarded as partially ordered phases. We can see from Figs. 4 and 6 that, continuous random magnetic field distribution can induce higher number of these partially ordered phases. Also it can be seen in Fig. 4 and 6 that, it is impossible to relate the magnetization values or widths of the constant ground state magnetization region of the partially ordered phases, with the system parameters.

When the temperature varies a little, these partially ordered phases disappear. This means that there have to be some first order transition lines ending with isolated critical points in Figs. 2 and 5. However in order to clarify whether this partially ordered phases are artifact or not of EFT based on DA, it is necessary to investigate the problem with more advanced methods.

We hope that the results obtained in this work may be beneficial form both theoretical and experimental point of view.

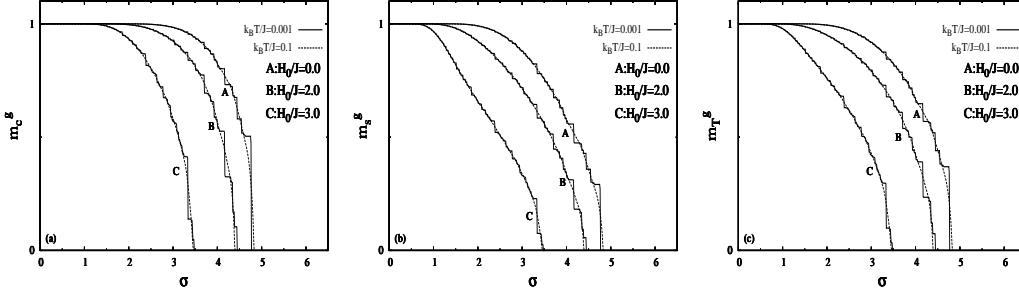


Figure 6: Variation of the ground state magnetizations with  $\sigma$  for some selected values of  $H_0/J$  for the system with double Gaussian magnetic field distribution. Each magnetization calculated at a temperature  $k_B T/J = 0.001$  can be regarded as ground state of the system. At the same time, the magnetization values calculated at the temperature  $k_B T/J = 0.1$  are plotted as dashed lines with the same  $H_0/J$  values. Fixed parameter values are  $r_2 = 1.0$  and  $r_3 = 1.0$ .

## 6 Appendix A: Symmetry properties of the coefficients

As seen in the definitions of the the coefficients given by (9), interchanging between certain indices do not change the part of that coefficient which is defined by (5). For obtaining the simple symmetry properties originated from this fact, let us start with the first coefficient by defining

$$K'_1(i, j, k, l) = \left[ \binom{4}{i} \binom{2}{k} \right]^{-1} K_1(i, j, k, l) = A_1^{5-i-l} A_3^{3-j-k} B_1^{i+l} B_3^{j+k}. \quad (15)$$

From the definition given in Eq. (5) we can see that Eq. (15) is invariant under the transformations  $i \rightarrow l, l \rightarrow i$  and  $j \rightarrow k, k \rightarrow j$ , thus we can use this property as

$$\begin{aligned} K_1(i, j, k, l) &= \binom{4}{i} \binom{2}{k} K'_1(i, j, k, l) \\ K_1(l, j, k, i) &= \binom{4}{l} \binom{2}{k} K'_1(i, j, k, l) \\ K_1(i, k, j, l) &= \binom{4}{i} \binom{2}{j} K'_1(i, j, k, l) \\ K_1(l, k, j, i) &= \binom{4}{l} \binom{2}{j} K'_1(i, j, k, l) \end{aligned} \quad (16)$$

i.e.,

$$\begin{aligned} K_1(l, j, k, i) &= \binom{4}{l} \binom{4}{i}^{-1} K_1(i, j, k, l) \\ K_1(i, k, j, l) &= \binom{2}{j} \binom{2}{k}^{-1} K_1(i, j, k, l) \\ K_1(l, k, j, i) &= \binom{4}{l} \binom{2}{j} \binom{4}{i}^{-1} \binom{2}{k}^{-1} K_1(i, j, k, l) \end{aligned} \quad (17)$$

Eq. (17) reduces the total number of coefficients which has to be calculated as separately from 60 to 45. In a similar way, for the other coefficients we can obtain similar symmetry properties as

$$K_2(i, k, j) = K_2(i, j, k) \quad (18)$$

$$K_3(i, k, j) = K_3(i, j, k) \quad (19)$$

$$K_4(l, i) = \binom{6}{l} \binom{2}{i} \binom{6}{i}^{-1} \binom{2}{l}^{-1} K_4(i, l) \quad (20)$$

These properties reduce the number of separate coefficients from 18 to 6, 27 to 9, 21 to 15, respectively. Thus for this system, total number of coefficients reduces from 126 to 75.

On the other hand, another important symmetry property of the coefficients which is useful in the calculations of the integration given in Eq. (5) is about the magnetic field. Let us choose  $P(H_i) = \delta(H_i - H_0)$  as a magnetic field distribution and denote the coefficient defined by Eq. (5) as  $\Theta_{klmn}(H_0, J_p, J_q) = A_p^k A_q^l B_p^m B_q^n$ . By writing hypergeometric functions in terms of the exponentials then writing them with binomial distribution and using Eq. (7) we get

$$\Theta_{klmn}(H_0, J_p, J_q) = \left(\frac{1}{2}\right)^{k+l+m+n} \sum_{r=0}^k \sum_{s=0}^l \sum_{t=0}^m \sum_{v=0}^n C_{rstv} f(H_0, a_p J_p + a_q J_q) \quad (21)$$

where

$$C_{rstv} = \binom{k}{r} \binom{l}{s} \binom{m}{t} \binom{n}{v} (-1)^{m+n-t-v} \quad (22)$$

and

$$a_p = 2r + 2t - m - k, \quad a_q = 2s + 2v - l - n \quad (23)$$

Now we can see from Eq. (21) that, for each term,  $C_{rstv} f(H_0, a_p J_p + a_q J_q)$  has a corresponding term which is  $C_{k-r, l-s, m-t, n-v} f(H_0, -a_p J_p - a_q J_q)$  in the sum. It can be seen from Eq. (22) that, these two coefficient are related to each other by

$$C_{k-r, l-s, m-t, n-v} = (-1)^{m+n} C_{rstv} \quad (24)$$

which means that for odd  $m+n$ , the terms which have  $f(H_0, a_p J_p + a_q J_q)$  and  $f(H_0, -a_p J_p - a_q J_q)$  are opposite signed coefficients. If  $m+n$  is even then the terms which have  $f(H_0, a_p J_p + a_q J_q)$  and  $f(H_0, -a_p J_p - a_q J_q)$  will be the same signed coefficients in the sum given in Eq. (21). Thus we can conclude that,

$$\Theta_{klmn}(H_0, -J_p, -J_q) = \begin{cases} \Theta_{klmn}(H_0, J_p, J_q), & m+n \text{ even} \\ -\Theta_{klmn}(H_0, J_p, J_q), & m+n \text{ odd} \end{cases} \quad (25)$$

Since the functions defined in Eq. (6) have the property  $f(H_i, x) = -f(-H_i, -x)$ , then we can write Eq. (25) as

$$\Theta_{klmn}(-H_0, J_p, J_q) = \begin{cases} -\Theta_{klmn}(H_0, J_p, J_q), & m+n \text{ even} \\ \Theta_{klmn}(H_0, J_p, J_q), & m+n \text{ odd} \end{cases} \quad (26)$$

Since the distribution given in Eq. (2) is symmetric about  $H_0 = 0$ , then in integration in Eq. (5) for any term  $\Theta_{klmn}(H_0, J_p, J_q)$  has a corresponding  $\Theta_{klmn}(-H_0, J_p, J_q)$  term. This means that in the case where random field distribution is given by Eq. (2),

$$\Theta_{klmn}(J_p, J_q) = \int dH_0 P(H_0) \Theta_{klmn}(H_0, J_p, J_q) \begin{cases} = 0, & m+n \text{ even} \\ \neq 0, & m+n \text{ odd} \end{cases} \quad (27)$$

is valid. Eq. (27) also reduces the number of the coefficients which has to be calculated, approximately half of the whole set of the coefficients.

## References

- [1] M. Ruhrig, B. Khamsehpour, K. J. Kirk, J. N. Chapman, P. Aitchison, S. McVitie, and C. D. W. Wilkinsons, *IEEE Trans. Magn.* **32**, 4452 (1996).
- [2] Th. Schrefl, J. Filder, K. J. Kirk, and J. N. Chapman, *IEEE Trans. Magn.* **33**, 4128 (1997).
- [3] Th. Schrefl, J. Filder, K. J. Kirk, and J. N. Chapman, *J. Magn. Magn. Mater.* **175**, 193 (1997).
- [4] B. Martinez, X. Obradors, L. Balcells, A. Rouanet, and C. Monty, *Phys. Rev. Lett.* **80**, 181 (1998).
- [5] G. V. Kurylanskaya, M. L. Sanchez, B. Hernando, V. M. Prida, P. Gorria, M. Tejedor, *Appl. Phys. Lett.* **82** (2003) 3053.
- [6] H. Zeng, J. Li, J. P. Liu, Z. L. Wang, S. Sun, *Nature* **420** (2002) 395.
- [7] C. Alexiou, A. Schmidt, R. Klein, P. Hullin, C. Bergemann, W. Arnold, *J. Magn. Magn. Mater.* **252** (2002) 363.
- [8] R. Skomski, *J. Phys. :Condens. Matter* **15** (2003) R841.
- [9] H. Schlorb, V. Haehnel, M. S. Khatri, A. Srivastav, A. Kumar, L. Schultz, S. Fahler, *Phys. Status Solidi B* **247** (2010) 2364.
- [10] J. E. Wegrowe, D. Kelly, Y. Jaccard, Ph. Guittienne, J. P. hAnsermet, *Europh Lett.* **45** (1999) 626.
- [11] A. Fert, L. Piraux, *J. Magn. Magn. Mater.* **200** (1999) 338.
- [12] R. H. Kodama, *J. Magn. Magn. Mater.* **200** (1999) 359.
- [13] S. J. Son, J. Reiche, B. He, M. Schuchman, and S. B. Lee, *J. Am. Chem. Soc.* **127**, 7316 (2005).
- [14] D. Lee, R. E. Cohen, and M. F. Rubner, *Langmuir* **23**, 123 (2007).
- [15] A. Hultgren, M. Tanase, C. S. Chen, D. H. Reich, *IEEE Transactions on Magnetism* **40** (2004) 2988.
- [16] A. Hultgren, M. Tanase, E. J. Felton, K. Bhadriraju, A. K. Salem, C. S. Chen, D. H. Reich, *Biotechnology Progress* **21** (2005) 509.
- [17] A. F. Bakuzis and P. C. Morais, *J. Magn. Magn. Mater.* **285**, 145 (2005).
- [18] V. S. Leite and W. Figueiredo, *Physica A* **350**, 379 (2005).
- [19] T. Kaneyoshi, *Phys. Status Solidi B* **242**, 2938 (2005).
- [20] T. Kaneyoshi, *J. Magn. Magn. Mater.* **321**, 3430 (2009).
- [21] T. Kaneyoshi, *Solid State Commun.* **152** (2012) 883
- [22] A. Zaim, M. Kerouad, and Y. El. Amraoui, *J. Magn. Magn. Mater.* **321**, 1077 (2009).
- [23] J. T. Ou, W. Lai, D. L. Lin, and F. Lee, *J. Phys. :Condens. Matter* **9**, 3687 (1997)
- [24] Huaiyu Wang, Yunsong Zhou, D. L. Lin, and Enge Wang, *Chin. J. Phys.* **39**, 85 (2001).
- [25] Huaiyu Wang, Yunsong Zhou, D. L. Lin, and Chongyu Wang, *Phys. Stat. Sol. (b)* **232**, 254 (2002).
- [26] Y. C. Su, R. Skomski, K. D. Sorge, D. J. Sellmyer, *Appl. Phys. Lett.* **84** (2004) 1525.
- [27] T. Kaneyoshi, *J. Magn. Magn. Mater.* **322**, 3014 (2010).

- [28] T. Kaneyoshi, J. Magn. Magn. Mater. **322**, 3410 (2010).
- [29] T. Kaneyoshi, Phys. Status Solidi B **248**, 250 (2011).
- [30] T. Kaneyoshi, Solid State Commun. **151** (2011) 1528.
- [31] E. Konstantinova, J. Magn. Magn. Mater. **320**, 2721 (2008).
- [32] T. Kaneyoshi, J. Magn. Magn. Mater. **323**, 1145 (2011).
- [33] T. Kaneyoshi, J. Magn. Magn. Mater. **323**, 2483 (2011).
- [34] T. Kaneyoshi, Physica A **390**, 3697 (2011).
- [35] M. Keskin, N. Şarlı, B. Deviren, Solid State Commun. **151** (2011) 1025.
- [36] S. Bouhou, I. Essaoudi, A. Ainane, M. Saber, F. Dujardin, J. J. de Miguel, J. Magn. Magn. Mater. **324** (2012) 2434
- [37] O. Canko, A. Erdiñç, F. Taşkın, M. Atış, Phys. Lett. A **375** (2011) 3547
- [38] N. Şarlı, M. Keskin, Solid State Commun. **152** (2012) 354.
- [39] Y. Yüksel, E. Aydiner, H. Polat, J. Magn. Magn. Mater. **323** (2011) 33168.
- [40] O. Canko, A. Erdiñç, F. Taşkın, A. F. Yıldırım, J. Magn. Magn. Mater. **324** (2012) 508
- [41] A. I. Larkin, Sov. Phys. JETP **31**, 784 (1970).
- [42] Y. Imry and S. K. Ma, Phys. Rev. Lett. **35**, 1399 (1975).
- [43] S. Fishman and A. Aharony, J. Phys. C **12**, L729 (1979).
- [44] J. L. Cardy, Phys. Rev. B **29**, 505 (1984).
- [45] T. Schneider and E. Pytte, Phys. Rev. B **15**, 1519 (1977).
- [46] A. Aharony, Phys. Rev. B **18**, 3318 (1978).
- [47] D. C. Mattis, Phys. Rev. Lett. **55**, 3009 (1985).
- [48] H.E. Borges and P.R. Silva, Phys. Stat. Sol. (b) **121** (1984) K19.
- [49] H.E. Borges and P.R. Silva, Phys. Stat. Sol. (b) **121** (1984) K25.
- [50] H. E. Borges and P. R. Silva, Physica A **144**,561 (1987).
- [51] A. Bobak, J. Karaba and L. Toth, Phys. Stat. Sol. (b) **155** (1989) K 143.
- [52] E. F. Sarmiento and T. Kaneyoshi, Phys. Rev. B **39**, 9555 (1989).
- [53] N. G. Fytas, A. Malakis, and K. Eftaxias, J. Stat. Mech. Theory Exp. (2008), 03015.
- [54] I. A. Hadjiagapiou, Physica A **389**, 3945 (2010).
- [55] N. Crokidakis and F. D. Nobre, J. Phys. Condens. Matter **20**, 145211 (2008).
- [56] O. R. Salmon, N. Crokidakis, and F. D. Nobre, J. Phys. Condens. Matter **21**, 056005 (2009).
- [57] R. M. Sebastianes and W. Figueiredo, Phys. Rev. B **46**,969 (1992).
- [58] T. Kaneyoshi, Physica A **139**, 455 (1985).
- [59] Ü. Akıncı, Y. Yüksel, H. Polat, Phys. Rev. E **83**, 061103 (2011).
- [60] D. P. Landau, H. H. Lee, and W. Kao, J. Appl. Phys. **49**, 1356 (1978).

- [61] J. Machta, M. E. J. Newman, and L. B. Chayes, *Phys. Rev. E* **62**, 8782 (2000).
- [62] N. G. Fytas and A. Malakis, *Eur. Phys. J. B* **61**, 111 (2008).
- [63] E. Albayrak and O. Canko, *J. Magn. Magn. Mater.* **270**, 333 (2004).
- [64] M. Gofman, J. Adler, A. Aharony, A. B. Harris, and M. Schwartz, *Phys. Rev. B* **53**, 6362 (1996).
- [65] R. Honmura, T. Kaneyoshi, *J. Phys. C* **12** (1979) 3979.
- [66] T. Kaneyoshi, *Acta Phys. Pol. A* **83** (1993) 703.
- [67] F. Zernike, *Physica* **7** (1940) 565.
- [68] Ü. Akıncı, Y. Yüksel, H. Polat *Phys. Rev. E* **83**, 061103 (2011)
- [69] Ü. Akıncı [arXiv:1205.3219v1](https://arxiv.org/abs/1205.3219v1) [cond-mat.stat-mech]